

THE MECHANICAL BEHAVIOR OF AISI H13 HOT-WORK TOOL STEEL PROCESSED BY SELECTIVE LASER MELTING UNDER TENSILE STRESS

Mei Wang^a, Yan Zhou^a, Q. S. Wei^a, Zhunfeng Fan^b

^a a State Key Laboratory of Materials Processing and Die & Mould Technology, School of
Materials Science and Technology, Huazhong University of Science and Technology, Wuhan
430074, P. R. China

^b b Department of Design Management , State Nuclear Demonstration Power Plant Co., Ltd.,
Weihai, 264300, P.R. China

Abstract

AISI H13 tool steel is commonly used in hot-working applications include die casting dies, inserts, forging dies, extrusion dies, etc. Molds fabricated by selective laser melting (SLM) with conforming cooling channels can maintain a steady and uniform cooling performance to the molding parts, which ensures high quality of the products and general reduction of the cycle time. Therefore, SLM process has gained increasing attention in the hot-work tool field. The present study concerns the properties of H13 materials that with and without preheating during the SLM process. X-ray diffraction (XRD), field emission scanning electron microscope (SEM), and high-temperature tensile tests were applied to investigate the phases, microstructures and resultant mechanical properties of SLM processed H13. Results show that the application of preheating during SLM process results in a more homogeneous microstructure of the material with better mechanical properties compared to those without preheating. High-temperature tensile strength increased from 1066 MPa to 1183 MPa, the total elongation increased from 5.7% to 8.1%. The high-temperature tensile strength of those parts with preheating was higher than those of the treated commercial H13 tool steel, while the total elongation was much lower than those commercial materials.

Introduction

AISI H13 is a 5% Cr ultrahigh-strength and secondary hardening steel, which exhibited good temper resistance, high hardness, and strength at elevated temperatures [1]. Its resistance to thermal fatigue, erosion, and wear has made it a commonly used hot-work tool steel on aluminum and magnesium die casting, extrusion and forging, as well as for many other hot-work applications. Currently, molds for hot-working applications are manufactured by combining manufacturing processes that include diecasting, forging, and subtractive CNC mechanical machining. It will lead to massive usage of materials and time wastage. Recently, the additive manufacturing technique has gained increasing attention [2, 3]. The layer-by-layer manufacturing offers the fabrication of high-density parts with complex geometry and a high degree of accuracy [4, 5]. Selective laser melting (SLM) is a typical AM technology that can fabricate high-density parts with complex geometrical designs [5-7]. It has been used in the production of molds [8, 9]. SLM processed molds with conformal cooling channels can maintain a steady and uniform cooling performance of the molds and thus ensuring high quality of the workpieces and general reduction of the cycle time [10]. Researchers have done a lot of work on the SLM processed H13 material. Pinkerton et al. compared the performance of SLMed parts fabricated by gas- and water-atomized powders [11]. They suggested that water-atomised H13 powders are a realistic alternative to the gas-atomised powders for direct laser additive manufacturing, giving

advantages in terms of material cost. Laakso et al. indicated that Design of Experiments (DOE) approach is a practical and reliable method for SLM processing optimization [12]. Holzweissig et al. studied the microstructure and mechanical performance of SLMed H13 [13]. They found that the microstructure after layerwise processing partially consisted of metastable-retained austenite which transformed to martensite in a subsequent tensile test. This improved the mechanical properties of the hot work tool steel enabling direct application. Mertens et al. investigated the influence of powder bed preheating on microstructure and mechanical properties [2]. They found that application of powder bed preheating resulted in a more homogeneous microstructure with better mechanical properties compared to H13 SLM parts produced without preheating. The fine bainitic microstructures lead to hardness values of 650 HV and ultimate tensile strength of 1965 MPa. Păcurar et al. took the processing parameters into account for the finite element analysis to improve the accuracy of molds [14]. They found that the technological parameters (power, scanning speed, preheating temperature) to be used within the SLM process have to be different, according to the type and the shape of the metallic tool to be manufactured. Safka et al. studied the influence of changes in building strategy to the properties of the parts [15]. They proposed that the different layering of the material lead to variation of mechanical properties in certain direction. Some studies have also studied on In-situ production to reinforce the original matrix with other powders. Nair et al. investigated the Ni-nanoparticles reinforced H13 steel produced by SLM [16]. They manufactured injection molds and found those molds fabricated with Ni/H13 showed excellent structural integrity, fine grain structure, and high hardness. AlMangour et al. investigated TiC/H13-steel-nanocomposite parts produced by SLM and observed enhanced mechanical and tribological properties [17]. AlMangour et al. investigated TiB₂/H13 steel nanocomposites produced by SLM. They applied hot isostatic pressing (HIP) post-treatment to improve the final density of the SLM fabricated component [18]. The hardness of the SLM-processed nanocomposite was found to be slightly higher relative to the unreinforced base metal, but friction and wear rate significantly decreased. The major pores were effectively eliminated in the nanocomposites and a further increase in the hardness values after HIP treatment because of the competition between the high-temperature annealing effect and the improvement in density. A slight increase in the wear rate after the post-treatment was observed as a result of the grain coarsening and agglomeration of the TiB₂ nanoparticles in the H13 matrix. Obviously, all studies above have investigated the effect of microstructures and properties of the part. No research concerned with the mechanical behavior of SLM processed H13 under the tensile stress at elevated temperature, which is an important index for the hot-work steel during its application [19].

2. Materials and experiments

As shown in Fig. 1, the supplied gas atomized alloyed powders (0.36 wt% C, 5.72 wt% Cr, 1.47 wt% Mo, 1.08 wt% Si, 1.07 wt% V, 0.68 wt% Mn, Fe balance) was in a spherical shape, with the average particle size of 25 μm . The oxygen content of powders is below 800 ppm. Powders were dried by vacuum for 4 h before the SLM processing. Wrought material (0.40 wt% C, 5.28 wt% Cr, 1.34 wt% Mo, 0.99 wt% Si, 0.98 wt% V, 0.385 wt% Mn, Fe balance) for tests was one AISI H13 type tool steel (8407 Supreme) supplied by the ASSAB company, which was oil quenched from 1020°C and double tempered at 525°C to a hardness of 579 HV.

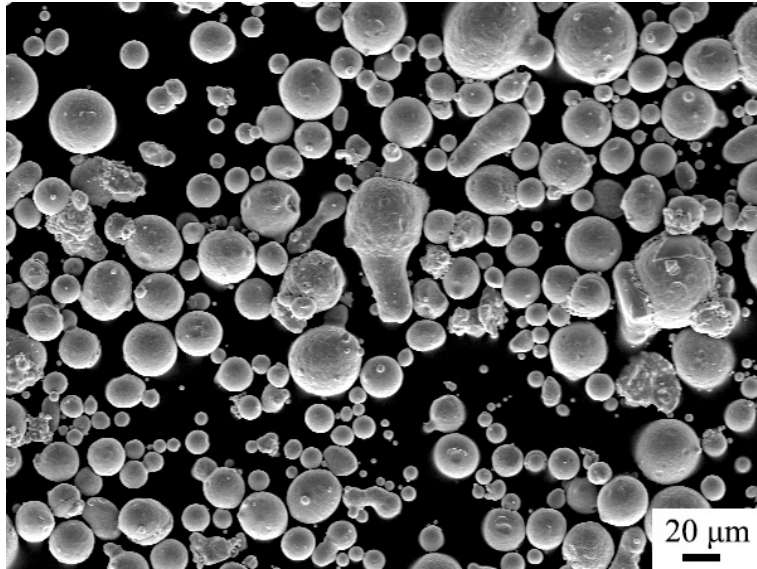
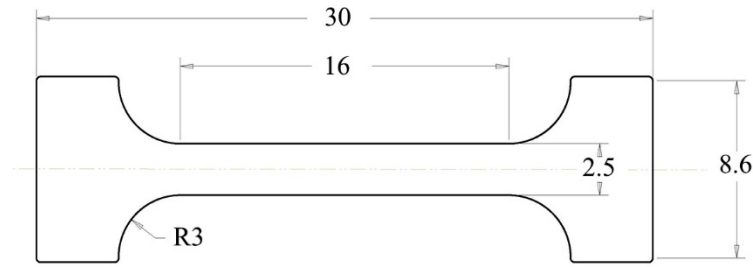


Fig. 1. SEM images of gas atomized alloyed powders.

Bulk materials were fabricated from the H13 powder by an SLM Solution machine. The layer thickness of the H13 powder was 40 μm , the laser power of 280 W, the scanning speed of 900 mm/s, the scanning spacing of 120 μm .

To identify the microstructural morphology and the phases existence after SLM processing, SEM and XRD were carried out. The microstructure observations were investigated by a scanning electron microscopy (FEI Quanta 650 FEG, America). Samples were ground to a 1200 grit and polished by an automatic polishing machine (Buehler Ecomet 200/Automet 300, America). Afterward, the samples were etched for 40 to 50 seconds in a water bath of 80°C. The etchant solution was prepared with 20 mL saturated picric acid, 0.1~0.2 mL hydrochloric acid and one drop of cleanser essence. Phase identification was performed by an XRD-7000s type machine (Shimadzu, Japan) with a Cu anticathode, $K\alpha$ radiation at 40 kV and 40 Ma. The 2θ is between 30° and 120°. All samples were ground to an 800 grit finish before the test. In order to characterize the mechanical properties due to microstructures evolution in the SLM process, hardness and tensile tests were employed. Hardness was tested by a Vickers hardness tester (Wolpert Wilson Instrument 432 SVD, China) at a load of 5 kg over 15 seconds of 6 identifications. Tensile specimens were CNC machined from the bulk materials according to Fig. 2. Tensile tests at 600°C were conducted by a Precision Universal tester machine (Shimadzu AG-IC 100 kN, Japan), with the strain rate of 1mm/min. Tensile tests for SLM processed H13 were load along the axes perpendicular to the building direction (BD) of SLM.



All dimensions are in mm.

Fig. 2. Tensile specimen profile.

3 Results and discussion

3.1 Phases analysis

As shown in Fig. 3, both SLM processed H13 with/without preheating parts show fcc and bcc phases. However, the wrought parts show only bcc phase. The 2 theta degree of (110) peak of α phase of the SLM processed H13 with/without preheating parts and the wrought parts were 44.7, 44.5, and 44.0 respectively. We explain the results with the Bragg's law,

$$2 d \sin\theta = n \lambda, (n=1, 2, 3\dots) \quad (1),$$

Where d is the lattice plane space, 2θ is the diffraction angle, λ is the wavelength, and n is a diffraction order. Obviously, the wrought H13 had the smallest lattice plane space according to the Bragg's law. This could attribute to the carbides precipitation from the matrix and stress relieve in the material after tempering treatment [20]. On the other side, at a preheating temperature of 200°C, fcc is higher present compared to those without preheating. During the cooling process for H13 material, austenite transforms to martensite when descends to a temperature about 300°C. Thus, the higher of the preheating temperature during SLM process, the fewer for martensite transformation. Therefore, there is more retained austenite present in the parts with preheating.

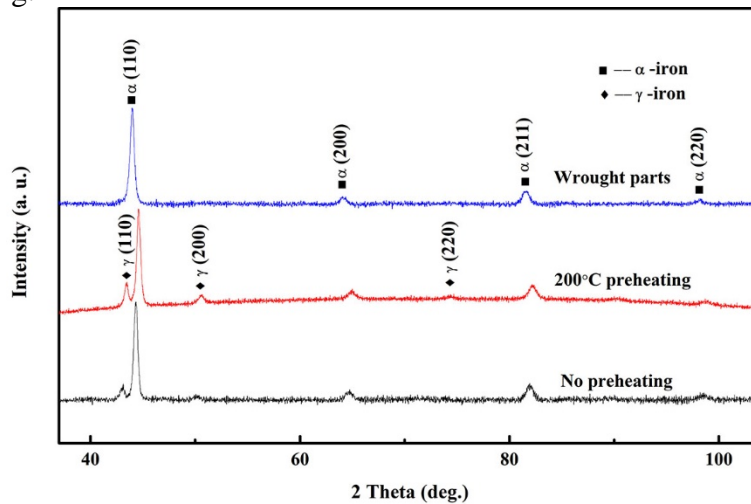


Fig. 3. The XRD spectra of H13 samples in the condition of SLM processed parts without preheating, with 200°C preheating, and wrought parts.

3.2 Microstructure investigation

Fig. 4 shows the SEM image of SLM processed parts with/without preheating and the wrought H13 parts. Fig. 4a and 4b both show the growth of cellular dendrite occurred epitaxially along the fusion line marked by the white dashed line which was taken from the top view (section perpendicular to the building direction) of the parts. No obvious difference in morphology for parts of with/without preheating SLM processed H13. While the wrought parts exhibited the prior austenite grains (marked by the white dashed lines) and lath martensite as revealed in Fig. 4c.

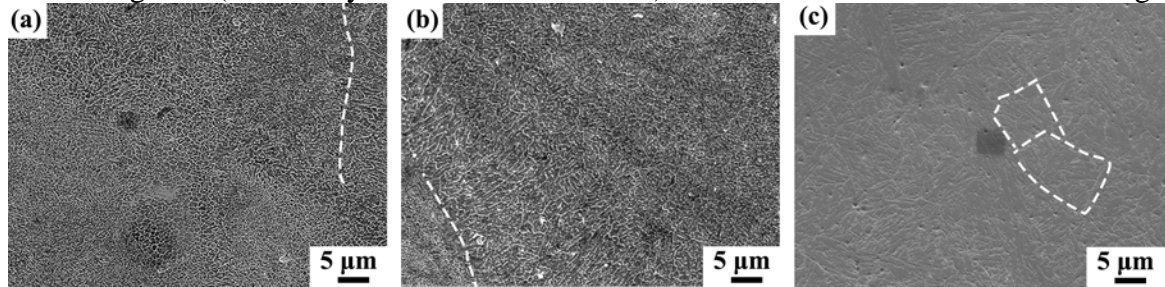


Fig. 4. SEM images of the H13 specimens of (a) without preheating, (b) 200°C preheating, and (c) wrought parts after austenitizing and tempering treatment.

3.3 Mechanical properties

Fig. 5 the high temperature (600°C) stress-strain curves of the SLM processed specimens with/without preheating as well as the wrought materials, the yield strength (YS, MPa), ultimate tensile strength (UTS, MPa) and total elongation (ϵ_{\max} , %) were determined and compared as shown in Table 1. The SLM processed samples without preheating exhibited the lowest UTS and the least ductility, the SLM processed samples with preheating had the highest YS and comparable UTS with the wrought parts, while the wrought parts showed the best ductility. Although the extremely fine martensite microstructure caused by the very high cooling rate during the SLM process generally leads to high hardness and tensile strength of the material. However, high residual stress originated by the SLM processed lead to the lower UTS and less ductility in the material. Therefore, those SLM processed H13 without preheating exhibited the largest hardness of 596 HV, but the least UTS value for brittle characters in the material. With a preheating temperature of 200°C, there was a larger amount of retained austenite in the material which leads to the lower hardness and less residual stress. Besides, the transformation from austenite to martensite lead to the compression stress during tensile tests, which together lead to the increase of the ductility in the material. When it concerns about the wrought parts, it should be noted a very good ductility in the material than all other SLM processed ones. This can be concluded from the fractography in Fig. 6. Though SLM processed H13 with/without preheating reveal the very fine dimples morphology in the magnified fracture surface (Figs. 6b and 6d), however Figs. 6a and 6c show the brittle fracture features of those materials which were in agreement with the performance of the tensile tests. Fig. 6e shows the ductility fracture features after tensile tests since a pronounced necking and a large percent reduction of the area are evident. Besides, a shear fracture in Fig. 6e begins at the interior (fiber zone) of the specimen and progresses to the surface. Fig. 6f reveals the conventional H13 material tear up under the tensile tests shows a large dimple fracture surface which caused by the precipitation of MnS particles (indicated by the blue circles). As published by the ASM hand book vol. 4 that wrought H13 need to be processed with series procedures before putting in an application [20]. Firstly, the austenitizing and fast cooling of the material to obtain a high hardness, and then the tempering treatment to obtain good toughness in the material. As a result, it must be practical that a similar

heat treatment should be used for SLM processed H13 to obtain comparable toughness in the material.

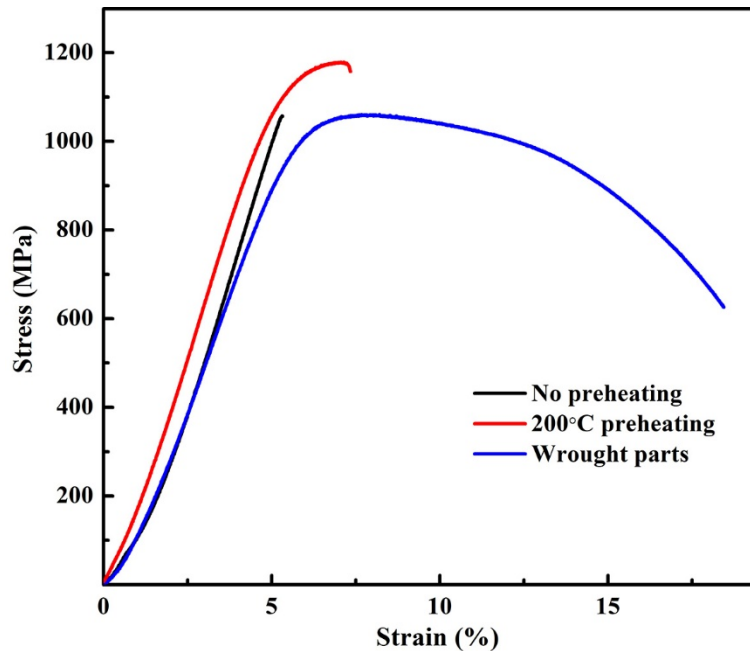


Fig. 5. Stress-strain curves of H13 samples in the condition of SLM processed parts without preheating, with 200°C preheating, and wrought parts from tensile tests at 600°C

Table 1. Summarized mechanical properties at 600°C

Condition	Hardness at room temperature, HV	Young's modulus, GPa	Yield strength, MPa	Ultimate tensile strength, Mpa	Total elongation, %
No preheating	596 ± 8.6	250	-	1066 ± 57.1	5.7 ± 0.41
With preheating	569 ± 9.1	215	1046 ± 4.3	1183 ± 15.9	8.1 ± 1.05
Wrought	579 ± 8.7	200	1002 ± 26.5	1125 ± 38.3	16.8 ± 1.24
*Wrought			825	1020	17.5

*Wrought is referred from ASM Vol. 1, which was tested at 595°C, and the material was oil quenched from 1010°C and double tempered at 527°C to 52 HRC.

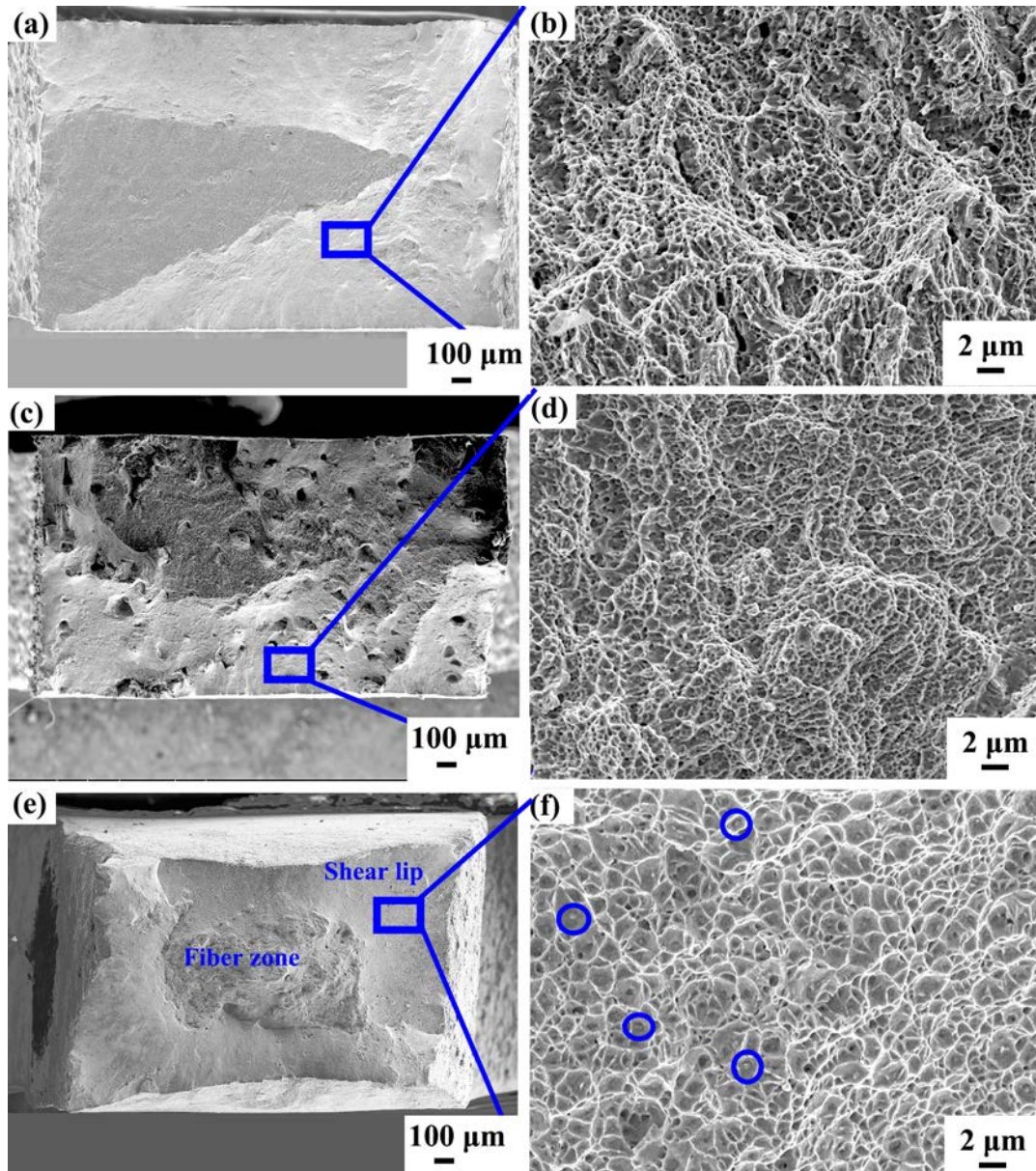


Fig. 6. SEM images of the fracture morphology of parts from tensile tests at 600°C. (a) and (b) are fracture surface of SLM processed H13 parts those without preheating. (c) and (d) are those with 200°C preheating. And (e) and (f) are wrought parts.

4. Conclusion

SLM is very powerful to manufactured geometrically complex structures. AISI H13 tool steel is suited well for processing by SLM. H13 that processed by SLM with/without preheating have been investigated, as well as those conventional wrought ones. The research results presented in the current study lead to the following conclusions:

- (1) The retained austenite was higher for SLM processed H13 with 200°C preheating than those without preheating.
- (2) The application of substrate preheating results in better mechanical properties compared to those without preheating. High-temperature tensile strength increased from 1066 MPa to 1183 MPa, the total elongation increased from 5.7% to 8.1%.

- (3) The high-temperature tensile strength of those parts with preheating was higher than those of the treated ASSAB 8407 Supreme tool steel, while the total elongation was much lower than those.

Acknowledgment

This work was supported by Fundamental Research Funds for the Central Universities (No. 2015ZDTD028), Hubei Science and Technology Innovation Project (No. 2014AAA020), Wuhan Key Technology Project (No. 2015010202010088) and the Academic Frontier Youth Team of Huazhong University of Science and Technology (HUST), Science and Technology Major Project of Guangdong Province (No. 2017B090911007), Science and Technology Major Project of Foshan City (No. 2016AG101253). The authors would also like to thank the State key Laboratory of Materials Processing and Die & Mould Technology, and the Analysis and Testing Center of HUST.

References

- [1] L.Y. Jia Z, Li J, et al., Crack growth behavior at thermal fatigue of H13 tool steel processed by laser surface melting, *International Journal of Fatigue* 78 (2015) 61-71.
- [2] R. Mertens, B. Vrancken, N. Holmstock, Y. Kinds, J.-P. Kruth, J. Van Humbeeck, Influence of Powder Bed Preheating on Microstructure and Mechanical Properties of H13 Tool Steel SLM Parts, *Physics Procedia* 83 (2016) 882-890.
- [3] G. Telasang, J. Dutta Majumdar, G. Padmanabham, M. Tak, I. Manna, Effect of laser parameters on microstructure and hardness of laser clad and tempered AISI H13 tool steel, *Surface and Coatings Technology* 258 (2014) 1108-1118.
- [4] J.-P. Kruth, B. Vandenbroucke, v.J. Vaerenbergh, P. Mercelis, Benchmarking of different SLS/SLM processes as rapid manufacturing techniques, *International conference Polymers & Moulds Innovations (PMI)*, Gent, Belgium (2005).
- [5] D. Wang, C. Song, Y. Yang, Y. Bai, Investigation of crystal growth mechanism during selective laser melting and mechanical property characterization of 316L stainless steel parts, *Materials & Design* 100 (2016) 291-299.
- [6] J.-P. Kruth, M. Badrossamay, E. Yasa, J. Deckers, L. Thijs, J. Van Humbeeck, Part and material properties in selective laser melting of metals, *Proceedings of the 16th international symposium on electromachining* (2010).
- [7] N. Read, W. Wang, K. Essa, M.M. Attallah, Selective laser melting of AlSi10Mg alloy: Process optimisation and mechanical properties development, *Materials & Design* (1980-2015) 65 (2015) 417-424.
- [8] M. Mazur, M. Leary, M. McMillan, J. Elambasserial, M. Brandt, SLM additive manufacture of H13 tool steel with conformal cooling and structural lattices, *Rapid Prototyping Journal* 22(3) (2016) 504-518.
- [9] A. Armillotta, R. Baraggi, S. Fasoli, SLM tooling for die casting with conformal cooling channels, *The International Journal of Advanced Manufacturing Technology* 71(1-4) (2014) 573-583.
- [10] D. Eric, Design considerations of conformal cooling channels in injection mould tools design: An overview, *Journal of Thermal Engineering* 1(7) (2015).

- [11] A.J. Pinkerton, L. Li, Direct additive laser manufacturing using gas- and water-atomised H13 tool steel powders, *The International Journal of Advanced Manufacturing Technology* 25(5-6) (2004) 471-479.
- [12] P. Laakso, T. Riipinen, A. Laukkanen, T. Andersson, A. Jokinen, A. Revuelta, K. Ruusuvoori, Optimization and Simulation of SLM Process for High Density H13 Tool Steel Parts, *Physics Procedia* 83 (2016) 26-35.
- [13] M.J. Holzweissig, A. Taube, F. Brenne, M. Schaper, T. Niendorf, Microstructural Characterization and Mechanical Performance of Hot Work Tool Steel Processed by Selective Laser Melting, *Metallurgical and Materials Transactions B* 46(2) (2015) 545-549.
- [14] R. Păcurar, A. Păcurar, N. Bâlc, Research on the Accuracy of Injection Molding Tools Made by H13 Material Using the Selective Laser Melting Technology, *Recent advances in Engineering Mechanics, Structures and Urban Planning* (2013).
- [15] J. Šafka, M. Ackermann, L. Voleský, Structural properties of H13 tool steel parts produced with use of selective laser melting technology, *Journal of Physics: Conference Series* 709 (2016) 012004.
- [16] R. Nair, W. Jiang, P. Molian, Nanoparticle Additive Manufacturing of Ni-H13 Steel Injection Molds, *Journal of Manufacturing Science and Engineering* 126(3) (2004) 637.
- [17] B. AlMangour, D. Grzesiak, J.-M. Yang, Nanocrystalline TiC-reinforced H13 steel matrix nanocomposites fabricated by selective laser melting, *Materials & Design* 96 (2016) 150-161.
- [18] G.D. AlMangour B, Yang J M., Selective laser melting of TiB₂/H13 steel nanocomposites: Influence of hot isostatic pressing post-treatment, *Journal of Materials Processing Technology* 244 (2017) 344-353.
- [19] A. Medvedeva, J. Bergström, S. Gunnarsson, J. Andersson, High-temperature properties and microstructural stability of hot-work tool steel, *Materials Science and Engineering: A* 523(1) (2009) 39-46.
- [20] A.I.H. Committee, *ASM Handbook–Volume 4: Heat Treating*, ASM International, Materials Park (1990) 33, 22-24.